

# Nanoporous Ultralow Dielectric Constant Organosilicates Templated by Triblock Copolymers

Shu Yang,<sup>\*,†</sup> Peter A. Mirau,<sup>‡</sup> Chien-Shing Pai,<sup>‡</sup> Omkaram Nalamasu,<sup>‡</sup> Elsa Reichmanis,<sup>†</sup> Janice C. Pai,<sup>†</sup> Yaw S. Obeng,<sup>§</sup> Joko Seputro,<sup>§</sup> Eric K. Lin,<sup>||</sup> Hae-Jeong Lee,<sup>||</sup> Jianing Sun,<sup>⊥</sup> and David W. Gidley<sup>#</sup>

Bell Laboratories, Lucent Technologies, 600 Mountain Avenue, Murray Hill, New Jersey 07974, Agere Systems, 600 Mountain Avenue, Murray Hill, New Jersey 07974, Agere Systems, 9333 S. John Young Parkway, Orlando, Florida 32819, National Institute of Standards and Technology, Polymers Division, 100 Bureau Drive, Gaithersburg, Maryland 20899-8541, and Departments of Materials Science and Engineering and Physics, University of Michigan, Ann Arbor, Michigan 48109

Received August 2, 2001. Revised Manuscript Received November 8, 2001

Triblock polymers, poly(ethylene oxide-*b*-propylene oxide-*b*-ethylene oxide) (PEO-*b*-PPO-*b*-PEO), are used as molecular templates in poly(methyl silsesquioxane) (MSQ) matrixes to fabricate nanoporous organosilicates for low dielectric constant applications. The results show that aggregation of block copolymers in the MSQ matrix can be prevented with the fast solvent evaporation which accompanies spin casting. Solid-state NMR shows that the triblock copolymer microphase-separates from the MSQ during a curing step, resulting in polymer domain size in the range of 3–15 nm, depending upon the polymer composition and loading percentage. When the films are heated to 500 °C, extremely small pores (2–6 nm) are generated, which are studied by small angle neutron scattering and positronium annihilation lifetime spectroscopy. These materials attain ultralow dielectric constants ( $k \approx 1.5$ ) with good electrical and mechanical properties.

## Introduction

Nanoporous or mesoporous materials have uses in many potential applications including membranes, sensors, waveguides, dielectrics, and microfluidic channels.<sup>1–5</sup> The control and understanding of the pore structure and properties at the nano- to micrometer length scale provides challenging opportunities for material scientists. Recently, in the microelectronics industry, demand for low dielectric constant ( $k$ ) materials has led to extensive efforts to explore the applicability of porous materials, especially nanoporous materials.<sup>6</sup> When the packing density between multilevel interconnects increases, RC delay, power consumption, and wire cross talk become major factors that limit device performance. A new low dielectric constant material is needed to

replace the current wire insulator: silicon dioxide ( $k \approx 4.0$ ). Since most solid materials have  $k > 3$ , ultralow- $k$  materials are prepared by introducing voids into the film and taking advantage of the low dielectric constant of air ( $k = 1$ ). Control over the pore size, shape, and distribution is critical to obtain materials with suitable mechanical and electrical properties to withstand the rigors required for the production of integrated circuits, especially when the device feature size is approaching 100 nm and the film is thin (less than 1  $\mu\text{m}$ ). Although it is possible to design ultralow dielectric constant materials, pore interconnectivity at high porosities makes it very difficult to meet the stringent requirements for ultralow- $k$  materials, including good thermal stability (above 400 °C), low moisture uptake, good mechanical strength, and high dielectric breakdown fields. Materials with homogeneous, nanometer-scaled, closed pores are preferred to preserve electrical and mechanical properties. In addition, these nanopores should be randomly distributed to ensure that the thin film properties are isotropic.

Porous silica with ordered structures as ultralow- $k$  materials have been fabricated through sol-gel processes.<sup>3,4</sup> Films with small pores (<10 nm) and  $k$  values that are less than 2.0 have been reported. However, it is not known whether films with porosities greater than 50% have the mechanical strength to withstand the chemical mechanical polishing (CMP) steps in the circuit fabrication process. Moreover, subsequent surface treatment and film-aging steps are required to minimize moisture absorption to the hydrophilic silica

\* To whom correspondence should be addressed.

<sup>†</sup> Bell Laboratories.

<sup>‡</sup> Agere Systems, Murray Hill, NJ.

<sup>§</sup> Agere Systems, Orlando, FL.

<sup>||</sup> National Institute of Standards and Technology.

<sup>⊥</sup> Department of Materials Science and Engineering, University of Michigan.

<sup>#</sup> Department of Physics, University of Michigan.

(1) Boyle, T. J.; Brinker, C. J.; Gardner, T. J.; Sault, A. G.; Hughes, R. C. *Comments Inorg. Chem.* **1999**, *20*, 209–231.

(2) Huo, Q. S.; Zhao, D. Y.; Feng, J. L.; Weston, K.; Buratto, S. K.; Stucky, G. D.; Schacht, S.; Schuth, F. *Adv. Mater.* **1998**, *9*, 974.

(3) Baskaran, S.; Liu, J.; Domansky, K.; Kohler, N.; Li, X. H.; Coyle, C.; Fryxell, G. E.; Thevuthasan, S.; Williford, R. E. *Adv. Mater.* **2000**, *12*, 291.

(4) Lu, Y. F.; Fan, H. Y.; Doke, N.; Loy, D. A.; Assink, R. A.; LaVan, D. A.; Brinker, C. J. *J. Am. Chem. Soc.* **2000**, *122*, 5258.

(5) Hedrick, J. L.; Miller, R. D.; Hawker, C. J.; Carter, K. R.; Volksen, W.; Yoon, D. Y.; Trollsas, M. *Adv. Mater.* **1998**, *10*, 1049.

(6) Miller, R. D. *Science* **1999**, *286*, 421.

surface. Hydrophobic organosilicates, such as poly(methyl silsesquioxane) (MSQ), are promising matrix materials for ultralow- $k$  dielectrics. They are structurally similar to inorganic silica and can be synthesized using similar chemistries. The bulky organic group reduces the density of the organosilicate, and the material becomes more hydrophobic. MSQ has a relatively low dielectric constant ( $k \approx 2.6$ – $2.8$ ), and a value of  $k \leq 2.0$  can be achieved in films with 30% porosity. For example, IBM researchers have reported that hyperbranched poly( $\epsilon$ -caprolactone) (PCL) with hydroxyl end groups has been used as a porogens to generate porous MSQ with a low dielectric constant and minimal moisture absorption.<sup>5,7</sup>

In contrast to the hydrophilic nature of silica, MSQ-based organosilicates change substantially during curing. The MSQ precursor is amphiphilic due to the presence of Si–OH groups and Si–CH<sub>3</sub> groups in the low molecular weight precursor. After polycondensation of the Si–OH groups to Si–O–Si linkages during the curing, MSQ becomes more hydrophobic. This change can alter the miscibility of the template material in solution and during the curing process, and templates with hydrophilic end groups may aggregate in the solution leading to macroscopic phase separation.<sup>8</sup> Also, if the MSQ matrix is not cured rapidly enough, macrophase separation between the template and the matrix could occur, resulting in a cloudy film and large pores. Clearly, a good understanding of the interactions between templates and organosilicates is essential for the design of nanoporous materials for ultralow- $k$  dielectrics. The understanding can further be applied to better design nanocomposites of organosilicates for applications in photonics, such as high  $\delta$  waveguides or electro-optic polymer modulators.

Block copolymers are good candidates for templates because they are known to microphase-separate into nanometer-sized domains.<sup>9</sup> Blocks with well-defined physical properties are tethered together, and the molecular weights, compositions, and architectures can be controlled to achieve the desired properties. Block copolymers have been widely used as compatibilizers, adhesives, additives, and surfactants to improve the miscibility of polymer blends.<sup>9</sup> When the ability of block copolymers to undergo self-assembly processes is taken advantage of, the properties of porous materials can be controlled at the molecular level through novel design, synthesis, and fabrication. Recently, they have been used as templates to fabricate bulk mesoporous inorganic and organic/inorganic hybrids with a variety of morphologies.<sup>10–13</sup>

Here, we report a new class of ultralow- $k$  materials with nanoporous structures. In this approach, amphiphilic triblock copolymers, poly(ethylene oxide-*b*-propy-

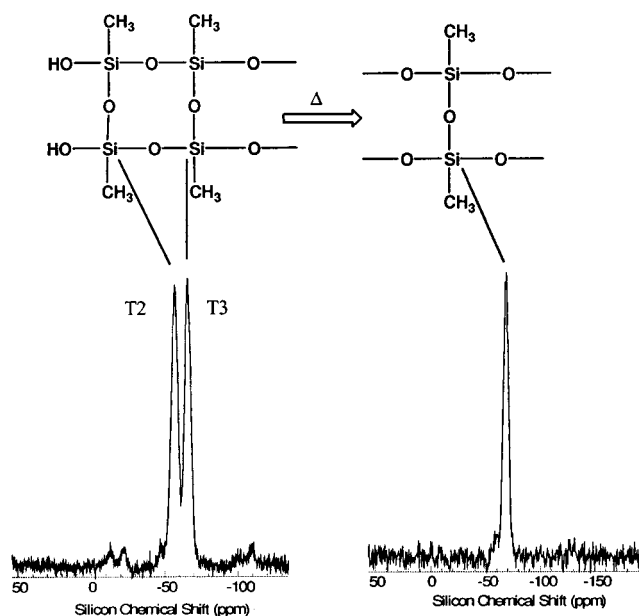


**Figure 1.** Chemical structures of MSQ precursor and cured MSQ.

lene oxide-*b*-ethylene oxide) (PEO-*b*-PPO-*b*-PEO), are used as molecular templates in a MSQ organosilicate matrix to generate nanopores. Both the template and the matrix are amphiphilic, so high-quality films can be prepared without macroscopic aggregation or precipitation. The MSQ matrix is then cured by slow heating to above 400 °C to promote polycondensation of the silicate matrix, followed by the calcination of block copolymers to generate pores. Small angle neutron scattering (SANS) and positronium annihilation lifetime spectroscopy (PALS) show that the pores are extremely small (2–6 nm). These nanoporous materials can attain ultralow dielectric constants ( $k \approx 1.5$ ) at 50% porosity with good electrical and mechanical properties. PALS studies show that the interconnectivity of the pores depends on the triblock copolymer loading and the percolation threshold is in the range of 20–25% of the mass fraction of the polymer.

## Experimental Section

**Materials.** Triblock copolymers of poly(ethylene oxide-*b*-propylene oxide-*b*-ethylene oxide) (PEO-*b*-PPO-*b*-PEO) (Pluronic F88 and P103) were obtained from BASF.<sup>14</sup> These two polymers have relative molecular masses of 11 400 and 4950 g/mol and PEO mass fractions of 80 and 30%, respectively. The MSQ precursor was obtained from Technoglas<sup>14</sup> as a solution with a mass fraction of 30% in *n*-butanol. The MSQ precursor has a  $M_{r,n}$  of 1668 g/mol and a polydispersity of 3.2 as measured by GPC. <sup>29</sup>Si NMR (Figure 1) shows that this precursor has a 1:1 ratio of silicon peaks corresponding to silicons attached to two and three Si–O–Si.

**Preparation of Ultralow- $k$  Materials.** Block copolymers were first dissolved in *n*-butanol, mixed with MSQ precursor, and passed through 0.45  $\mu$ m PTFE filters. The films for capacitance measurement were spun on Si wafers coated

(7) Nguyen, C. V.; Carter, K. R.; Hawker, C. J.; Hedrick, J. L.; Jaffe, R. L.; Miller, R. D.; Remenar, J. F.; Rhee, H.-W.; Rice, P. M.; Toney, M. F.; Trollsas, M.; Yoon, D. Y. *Chem. Mater.* **1999**, *11*, 3080.

(8) Alexandridis, P.; Holzwarth, J. F.; Hatton, T. A. *Macromolecules* **1994**, *27*, 2414.

(9) Hamley, I. W. *The Physics of Block Copolymers*; Oxford University Press: Oxford, 1998 and references therein.

(10) Templin, M.; Franck, A.; DuChesne, A.; Leist, H.; Zhang, Y. M.; Ulrich, R.; Schadler, V.; Wiesner, U. *Science* **1997**, *278*, 1795.

(11) Yang, P. D.; Zhao, D. Y.; Chmelka, B. F.; Stucky, G. D. *Chem. Mater.* **1998**, *10*, 2033.

(12) Zhao, D. Y.; Huo, Q. S.; Feng, J.; Melosh, N.; Fredrickson, G. H.; Chmelka, B. F.; Stucky, G. D. *Science* **1998**, *279*, 548.

(13) Chan, V. Z.-H.; Hoffman, J.; Lee, V. Y.; Iatrou, H.; Avgeropoulos, A.; Hadjichristidis, N.; Miller, R. D.; Thomas, E. L. *Science* **1999**, *286*, 1716.

(14) Certain commercial equipment and materials are identified in this paper to adequately specify the experimental procedure. In no case does such identification imply recommendation by the National Institute of Standards and Technology nor does it imply that the material or equipment is necessarily the best available for this purpose.

with TiN (300 Å Ti and 1000 Å TiN deposited on Si wafers subsequently) at 2000–3000 rpm for 30 s at room temperature and baked on a hotplate at 120 °C for 0.5 h in ambient air. The films were then placed in a tube furnace purged under N<sub>2</sub>. After they were soaked in N<sub>2</sub> for more than 1 h, the furnace temperature was ramped at a heating rate of 1.5 °C/min to 500 °C and held at this temperature for 2 h before being cooled slowly. The final film thickness was 0.3–0.8 μm depending on the solution concentration and spin speed. The thickness was measured by Dektak<sup>3</sup>-30 surface profiler with results that were comparable to the results from ellipsometry (J. A. Wollam Co.). The thickness of the films spun on Si wafers was measured on a Nanometrics 210XP Visible (Nanometrics Inc.). The samples for solid-state NMR measurement were powders scraped from thin films spun on Si wafers and cured at 120 °C for 12 h. The samples for specular X-ray reflectivity (XR) and SANS studies were prepared as described before on 4-in. (100) Si wafers with thickness larger than 0.5 μm. Smaller pieces from the same samples were used in the PALS studies.

**Characterization.** The solid-state proton NMR experiments were performed at 400 MHz by using a Varian Unity NMR spectrometer with a 4 mm magic angle spinning probe and the spinning speed regulation at 12 kHz. The proton pulse widths were 3.5 μs, and the dipolar filter pulse sequence<sup>15</sup> was used to measure the chain dynamics and for the spin diffusion experiments. The elemental compositions of low-*k* materials were analyzed by Galbraith Laboratories, Inc. Due to the high percentage of Si in the film, the composition of oxygen was not measured. Instead, it was calculated by subtracting the compositions of C, H, and Si from 100%. The curing of the MSQ precursor was monitored by a Nicolet Magna-IR 560 spectrometer and <sup>29</sup>Si NMR. The thermal decomposition of triblock copolymers was studied by means of a Perkin-Elmer thermogravimetric analyzer TGA 7 under nitrogen flow. The thermal transition temperatures were monitored by a Perkin-Elmer differential scanning calorimeter DSC 7.

The morphology of the dielectric film was imaged from the cross section obtained by TEM. The ultrathin films (~50 nm) were first cut by focused ion beam (FIB) milling.<sup>16</sup> They were then lifted out and transported to a carbon-coated copper grid for TEM analysis.

**Electrical Properties.** The capacitance of the film was measured between Al (top) and TiN (bottom) electrodes at room temperature in air by the use of a 4284A precision LCR meter at a frequency of 1 kHz. Aluminum dots, with diameters of 3 mm, were vapor-deposited through a shadow mask on the film after the thermal treatment. The capacitance measurement was averaged on four dots. The dielectric breakdown strength was measured on a 4145B Hewlett-Packard (HP) semiconductor parameter analyzer with the same sample setups. The current–voltage curve was obtained with a maximum sweep voltage of 100 V.

**Pore Size, Density, and Interconnectivity.** Specular XR was measured using a  $\theta$ – $2\theta$  configuration with a fine focus copper X-ray tube as the radiation source. The data were collected at grazing incident angles, ranging from 0.01 to 1.0°, to determine the density of the overall dielectric film.<sup>17</sup> The wall density of the pores and pore sizes were measured by SANS conducted on the NG1 and NG3 instruments at the Center for Neutron Research at the National Institute of Standards and Technology (NIST).<sup>17</sup> A 4-in. (100) Si wafer was diced into more than six round pieces, each with a diameter of 1.7 cm, and they were stacked together to enhance the scattering intensity.

The pore size was also measured by PALS<sup>18</sup> at room temperature. The uncapped samples were studied at two implantation energies, 5.0 and 1.0 keV, to search for any

depth-related heterogeneity. When open porosity of the films was detected, an 80 nm silica cap was deposited to confine Ps to the pores in the film, which allowed for the measurement of the intrinsic pore size in an interconnected porous network.

**Mechanical Properties.** Young's modulus and hardness were measured by frequency specific depth-sensing indentation on a Nanoindenter XP as described in the literature.<sup>19</sup> The system has a load and displacement resolution of 0.3 μN and 0.16 nm, respectively. The data were obtained at the displacement depth of 75 nm of the films spun on Si wafers and averaged over nine indents. Fused glass was used as reference material.

## Results and Discussion

Amphiphilic PEO-*b*-PPO-*b*-PEO triblock copolymers have been extensively studied as polymeric surfactants and self-assembled systems with a complex phase diagram.<sup>8,11,20</sup> We have used two of the block copolymers, Pluronic F88 and P103, as templates to prepare low dielectric constant films. The samples were prepared by the dissolving of polymers in *n*-butanol, followed by mixing with a MSQ precursor. The solution was then spun onto (100) Si wafers, followed by baking and curing steps to lock the polymer into the MSQ matrix.

Polymer chain conformation and dynamics in the composite are important factors that will affect the miscibility and domain size. In DCS, the bulk F88 has a melting point at 61 °C, which is associated with a semicrystalline morphology for the PEO domains. These semicrystalline domains are not observed in the spin-coated film by fast magic angle spinning NMR or DSC. Both PPO and PEO chains are mobile in the composites, and the crystallization of PEO is suppressed in the composites. The high mobilities for both the PEO and PPO blocks ( $T_g$ 's ≈ –70 °C) allow the polymer chains to self-organize rapidly and microphase-separate from the matrix during curing. The fast evaporation of solvent by spin-coating followed by matrix cross-linking restricts further aggregation and macroscopic phase separation of block copolymers, resulting in a clear film. Fast magic angle spinning and 2D spin exchange NMR show that the block copolymers form core-shell structures with the PPO block at the polymer–matrix interface.<sup>21,22</sup> In comparison, a cloudy film is always obtained when the solution is evaporated slowly, suggesting that the block copolymers aggregate and precipitate when the MSQ becomes hydrophobic. In the cloudy film of the F88 composite, a melting point of 51 °C was always observed in DSC.

The polymer domain size and the polymer–MSQ interaction define the final pore size and structure. A dipolar filter pulse sequence followed by a spin diffusion delay time<sup>15</sup> has been used to probe the molecular dynamics of the triblock copolymer and methyl silsesquioxane in the composites and to measure the length scale of phase separation.<sup>23,24</sup> The domain sizes were measured by using established procedures<sup>24</sup> in static

(15) Egger, N.; Schmidtrohr, K.; Blumich, B.; Domke, W. D.; Stapp, B. *J. Appl. Polym. Sci.* **1992**, *44*, 289.

(16) Giannuzzi, L. A.; Drown, J. L.; Brown, S. R.; Irwin, R. B.; Stevie, F. A. In *Specimen Preparation for Transmission Electron Microscopy of Materials IV. Materials Research Society Symposium Proceedings Vol. 480*; Anderson, R. M., Walck, S. D., Eds.; Materials Research Society: Pittsburgh, PA, 1997; pp 19–27.

(17) Wu, W. L.; Wallace, W. E.; Lin, E. K.; Lynn, G. W.; Glinka, C. *J. J. Appl. Phys.* **2000**, *87*, 1193.

(18) Gidley, D. W.; Frieze, W. E.; Dull, T. L.; Sun, J.; Yee, A. F.; Nguyen, C. V.; Yoon, D. Y. *Appl. Phys. Lett.* **2000**, *76*, 1282.

(19) Oliver, W. C.; Pharr, G. M. *J. Mater. Res.* **1992**, *7*, 1564.

(20) Schmolka, I. R. *J. Am. Oil Chem. Soc.* **1977**, *54*, 110.

(21) Yang, S.; Mirau, P.; Pai, C.-S.; Nalamasu, O.; Reichmanis, E.; Lin, E. K.; Lee, H.-J.; Gidley, D. W.; Sun, J. *Chem. Mater.* **2001**, *13*, 2762.

(22) Mirau, P. A.; Yang, S. *Chem. Mater.* **2001**, in press.

(23) Clauss, J.; Schmidtrohr, K.; Spiess, H. W. *Acta Polym.* **1993**, *44*, 1.

(24) VanderHart, D. L.; McFadden, G. B. *Solid State Nucl. Magn. Reson.* **1996**, *7*, 45.

**Table 1. Domain Sizes for Polymer/MSQ Spun on Wafers with Different Mass Fractions Measured by Solid-State  $^1\text{H}$  NMR<sup>a</sup>**

polymer loading %	dimensionality <sup>b</sup>	<i>d</i> (nm)	<i>d</i> <sub>p</sub> (nm)
F88	3	6.1	8.8
F88/MSQ, 15	3	3.7	6.2
F88/MSQ, 20	3	5.3	7.9
F88/MSQ, 30	2	7.2	12.5
F88/MSQ, 40	2	7.5	11.3
F88/MSQ, 50	2	10.3	13.9
P103/MSQ, 15	3	2.9	4.8
P103/MSQ, 30	2	3.5	6.2
P103/MSQ, 40	2	7.3	8.8
P103/MSQ, 50	2	14.3	19.3

<sup>a</sup> The domain size of bulk P103 was not measured because it is a paste at room temperature. <sup>b</sup> Based on PALS results.

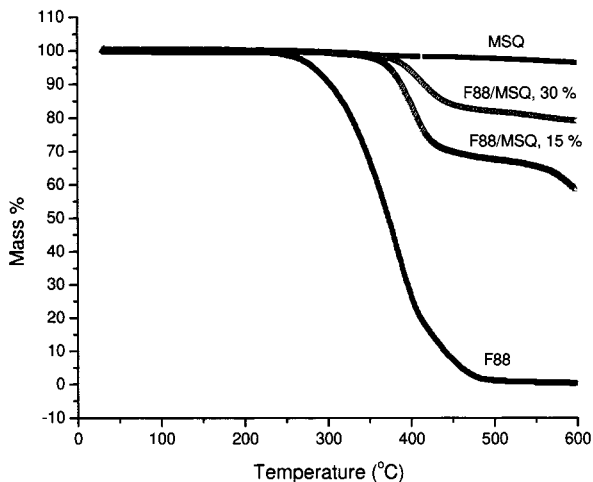


**Figure 2.** TGA of F88, MSQ, and mixture of F88 with MSQ at different mass fractions. The heating rate is 10 °C/min under N<sub>2</sub>.

samples using 10 cycles of the dipolar filter with a 20 ms delay between pulses to saturate the signals from the MSQ. This procedure can be used to estimate the distance *d* across the minor phase and the overall repeat distance or long period *d*<sub>p</sub> (see Table 1). It is notable that the bulk triblock copolymer exhibits larger domains of PPO within a matrix of PEO while the nanocomposite possesses smaller domains with PEO in the center and PPO at the polymer–MSQ interface. For a nanocomposite with an F88 mass fraction of 15%, *d* and *d*<sub>p</sub> are 3.7 and 6.2 nm, respectively. In comparison, the bulk F88 has a PPO domain size of 6.1 nm and a long period of 8.8 nm. The small domain size is a critical feature of the MSQ composites and is controlled by the polymer loading fraction.

After the spun film was baked at 120 °C to remove the solvents, it was then heated slowly to 500 °C and held at this temperature for 2 h in N<sub>2</sub>. Thermogravimetric analyses (TGA) showed that the neat triblock copolymers began to decompose at 240 °C at a heating rate of 10 °C/min and were completely removed above 500 °C or after soaking at 400 °C for 1 h under N<sub>2</sub> (see Figure 2). The mixtures of F88/MSQ with F88 mass fractions of 15 and 30% had a mass loss of less than 1% below 300 °C at a heating rate of 10 °C/min. With the use of this procedure, the MSQ precursors were cured by the slow heating without decomposition of polymers and large-scale phase separation of the block copolymers was inhibited by the covalent structure of the matrix.

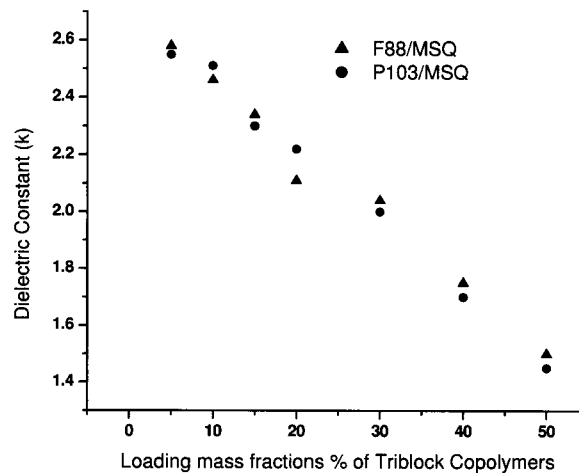


**Figure 3.** Relationship of dielectric constant vs loading mass fraction of triblock copolymers in MSQ.

The mass loss increased dramatically when the temperature was above 350 °C, as shown in Figure 2. When temperatures were greater than 500 °C, more than 18 and 32% of mass losses were observed in these mixtures with F88 mass fractions of 15 and 30% in MSQ, respectively (see Figure 2). The TGA data show that the decomposition temperature of polymer in MSQ is higher than that of the bulk material.

**Electrical Properties.** After decomposition of the polymers, pores are introduced in MSQ. In Figure 3, the dielectric constant decreases from 2.6 to 2.8 to 1.5 as the mass fraction of F88 or P103 increases to 50%. Although the dielectric constant depends on the film porosity, the dielectric breakdown strength may be strongly affected by the size and shape of the pore as well as by whether it is closed or open. In the thin low-*k* film, a small voltage can lead to a large electric field on the device.

The current–voltage (*I*–*V*) curves have been measured for MSQ and porous films with different polymer loadings between 3 mm Al (top) and TiN (bottom) electrodes at room temperature. The applied voltage was ramped from 0 to 100 V at a step of 5 V/s. The results show that the porous MSQ films with thickness ranging from 0.3 to 0.8 μm have a very high breakdown field (>2 MV/cm).<sup>21</sup> At 0.5 MV/cm, the leakage current density is on the order of 10<sup>−8</sup> to 10<sup>−9</sup> A/cm<sup>2</sup> for porous MSQ films. Within experimental error, it is similar to that of cured MSQ. A high breakdown field is important for practical applications of thin films, and better leakage currents are expected with films prepared in a clean room environment. Since these films are not preannealed or capped before the measurements, the high breakdown field indicates that these films have either closed pores or pores smaller than the mean free path of air (≈60 nm).<sup>25</sup> Cross-sectional TEM revealed no visible pores in the films with F88 mass fractions of 30%. Some isolated pores (≈5–10 nm) were observed in the film with a F88 mass fraction of 50%, but these pores represented only a small fraction of the total

(25) Jain, A.; Rogojevic, S.; Nitta, S. V.; Pisupatti, V.; Gill, W. N.; Wayner, P. C., Jr.; Plawsky, J. L.; Standaert, T. E. F. M.; Oehrlin, G. S. *Low-Dielectric Constant Materials V. Materials Research Society Symposium Proceedings Vol. 565*; Hummel, J., Endo, K., Lee, W. W., Mills, M., Wang, S.-Q., Eds.; Materials Research Society: Warrendale, PA, 1999; p 29.

**Table 2. Physical Properties of Porous Ultralow-*k* Materials with Different Polymer Mass Fractions in MSQ Measured by XR and SANS**

film	overall density (g/cm <sup>3</sup> )	wall density (g/cm <sup>3</sup> )	porosity (%)	avg chord length (nm)
MSQ	1.3	N/A	0	N/A
F88/MSQ, 30%	0.88 ± 0.02	1.16 ± 0.16	24 ± 9	1.4 ± 0.3
F88/MSQ, 40%	0.65 ± 0.02	1.19 ± 0.13	45 ± 6	3.5 ± 0.4
F88/MSQ, 50%	0.46 ± 0.02	0.99 ± 0.14	53 ± 6	5.2 ± 0.7
P103/MSQ, 30%	0.86 ± 0.02	1.18 ± 0.27	27 ± 17	1.6 ± 0.5
P103/MSQ, 40%	0.52 ± 0.02	1.03 ± 0.15	50 ± 7	4.6 ± 0.6
P103/MSQ, 50%	0.42 ± 0.02	0.98 ± 0.16	57 ± 6	6.3 ± 1.0

porosity measured by other means. It has been found to be difficult to visualize very small pores using TEM.

#### Thin Film Density, Pore Size, and Porosity.

Here, we use a combination of XR and SANS (XR/SANS)<sup>17</sup> and PALS<sup>18</sup> to nondestructively measure the nanometer-sized pore structure of the film. In comparison to TEM, XR/SANS and PALS can more quantitatively study the porosity (*P*), average pore size, and pore size distribution of these low-*k* materials as processed on silicon wafers. In addition, PALS is very sensitive to micropores and the pore interconnectivity. The density of the overall film and pore wall density ( $\rho_w$ ) are important to the mechanical strength of the porous films and can be monitored by specular XR.

Single-crystal silicon wafers are essentially transparent to neutrons, and scattering arises primarily from the pore structure. By fitting the SANS data with the random two-phase Debye model, assuming that the film has the elemental composition of the cured MSQ resin, and measuring the average film density from XR, we determine the pore size, porosity, density of the overall dielectric film, and pore wall density (see Table 2). For porous F88/MSQ, the overall density and wall density decrease to  $0.46 \pm 0.02$  and  $0.99 \pm 0.14$  g/cm<sup>3</sup>, respectively, as the porosity increases to  $53 \pm 6\%$ . For porous P103/MSQ, the overall density and wall density decrease to  $0.42 \pm 0.02$  and  $0.98 \pm 0.16$  g/cm<sup>3</sup>, respectively, as the porosity increases to  $57 \pm 6\%$ . These data are presented with the standard uncertainty of the measurements. The pore sizes (the average chord length of the two-phase material) are found to be extremely small, which are  $1.4 \pm 0.3$  and  $1.6 \pm 0.5$  nm, respectively, for porous MSQ with mass fraction of 30% F88 and P103, respectively.

These small pore sizes are close to the lower limit of the SANS probing capability but are well within the sensitivity of PALS. When positronium (Ps) is formed within an insulator, it tends to localize in open-volume pores. The reduced Ps annihilation lifetime is associated with the average pore size as measured by its mean free path (which should be the same as the average chord length from SANS). The pore interconnectivity (open vs closed) can be deduced from the intensity and lifetime of Ps that diffuses through the film and escapes into vacuum. When interconnected pores are detected, an 80 nm silica cap is deposited to confine Ps to the pores in the film. For interconnected pores, a two-dimensional tubular pore model is used, whereas for isolated pores, a three-dimensional cubic pore model is used for fitting. Micropores in the range of 6–11 Å in diameter are always detected and appear to be characteristic of the MSQ matrix. At mass fractions of 30% F88 and P103,

the average pore sizes are  $2.7 \pm 0.2$  and  $3.5 \pm 0.2$  nm, respectively. These values correlate well with the pore sizes obtained from SANS and are consistent with the domain sizes measured by solid-state NMR. The pore size increases with the loading of triblock copolymers, and the data from SANS and PALS are compared in Table 3. At a loading of 50% F88, the pore sizes remain small:  $5.2 \pm 0.7$  nm from SANS and  $4.8 \pm 0.3$  nm from PALS measurements.

**Percolation Threshold.** In addition to pore size, the pore interconnectivity is an important material parameter that will affect the electrical and mechanical properties of the film. Large and open pores make the thin film more susceptible to metal diffusion that could adversely affect the electrical or mechanical properties as well as the adhesion to the interface. However, high breakdown strength does not necessarily mean that the pores are closed and it is difficult to draw a conclusion on pore structure by *I*–*V* measurement. In comparison, beam PALS is very sensitive to the pore distribution and interconnectivity in novel low-*k* materials. The pore interconnectivity can be determined from the intensity of the Ps vacuum component of the uncapped samples. The intensities of the Ps annihilations in the film ( $I_0$ ) and in a vacuum ( $I_{\text{vacuum}}$ ) are plotted in Figure 4. The Ps in a vacuum starts to increase and the Ps in the film decreases at a F88 mass fraction of 25%, which is therefore considered to be the percolation threshold (more precisely the threshold is in the range of mass fractions of 20–25%). At this threshold, the mesopores start to merge with or connect to surrounding pores and the diffusion length of Ps increases, enabling some of the Ps to escape into vacuum. We consider the porous structure to be partially interconnected at this composition, and the interconnectivity increases with polymer loadings. As the F88 mass fraction increases to 40 or 50%, the porous network is totally interconnected because nearly all the Ps in the mesopores escape into vacuum. The small fraction of Ps remaining in the film is believed to arise from Ps in closed micropores. Polymer loading at a mass fraction of 40% is an upper limit on the loading required for 100% pore interconnection. The pores might be 100% interconnected at 30% loading, but some Ps is still annihilated in the film before it is able to diffuse out. The leakage current is found to increase when pores are interconnected above 25% of the mass loadings of polymers; however, the high breakdown strength is not greatly affected. It is believed that it is due to the small average pore size, 3–5 nm, in the films compared to the mean free path of air ( $\approx 60$  nm).<sup>25</sup>

**Mechanical Properties.** High mechanical strength in low dielectric constant films is essential for the circuit integration process. The use of SiO<sub>2</sub> as a dielectric insulator for such a long time is due in part to its good mechanical properties. It has a density of 2.0–2.2 g/cm<sup>3</sup> and a Young's modulus of  $\approx 77$  GPa.<sup>26</sup> Compared to SiO<sub>2</sub>, low-*k* materials have lower densities and mechanical strength. Design and synthesis of a low-*k* material with a high Young's modulus and hardness remains a significant challenge.

The preparation of MSQ with extremely small pores makes it possible to have ultralow dielectric constant

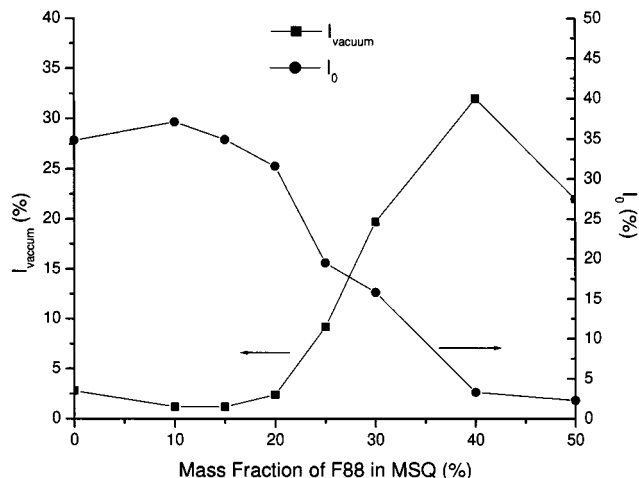
(26) Ryan, E. T.; Fox, R. J. I. *Future Fab International* **2000**, 8, 169.

**Table 3. Comparison of Pore Sizes Measured by XR/SANS and PALS on Films from F88/MSQ with Different Loadings**

polymer loading mass fractions (%)	0	15	30	40	50
avg chord length (nm) (SANS)	N/A	N/A	1.4 ± 0.3	3.5 ± 0.4	5.2 ± 0.7
pore size (nm) (PALS)	0.6–1.1	2.2 ± 0.2	2.7 ± 0.2	4.5 ± 0.3	4.8 ± 0.3

**Table 4. Mechanical Strength of Various Porous Films**

mechanical strength	MSQ	P103/MSQ, 30%	F88/MSQ, 30%	F88/MSQ, 40%	F88/MSQ, 50%
Young's modulus (GPa)	5.8 ± 1.0	2.7 ± 0.4	3.0 ± 0.3	1.3 ± 0.1	0.6 ± 0.1
hardness (GPa)	1.3 ± 0.4	0.5 ± 0.1	0.6 ± 0.1	0.28 ± 0.03	0.16 ± 0.02

**Figure 4.** Percolation threshold of porous MSQ templated by F88.

materials with good mechanical properties. The Young's modulus and hardness of our ultralow- $k$  materials have been measured by nanoindentation and are listed in Table 4. Depending on the penetration depth of indenter, the Young's modulus and hardness of thin films could vary over a large range due to the competition between "skin" and "substrate" effects. All the data were taken at a probe penetration depth of 75 nm into the dielectric films, and the reported results were averaged on nine spots. To minimize errors associated with potential nanoscale variabilities, fused glass was used as a reference material (a Young's modulus of 58 GPa and hardness of 5.4 GPa, respectively). In the porous film with 30% porosity, the Young's modulus and hardness are only reduced to half of that of the neat MSQ:  $\approx 3$  GPa and 0.5–0.6 GPa, respectively, compared to 6 and 1.3 GPa of the MSQ matrix (see Table 4). The films templated by a mass fraction of 50% triblock copolymer do not collapse after thermal treatment,

indicating both good mechanical strength and adhesion to the substrate. In comparison, the films templated by the same mass fraction of random copolymers completely collapsed on 4-in. Si wafers after the thermal treatment. The unique characteristics of triblock copolymers allow us to tailor the phase behavior and domain size of the nanocomposite, resulting in small pores in the film that are needed to withstand more applied forces.

### Conclusions

A new class of nanoporous organosilicates with dielectric constants as low as 1.5 has been designed using the self-assembly of triblock copolymers. Solid-state NMR studies show that the triblock copolymer microphase-separates in the MSQ with a domain size in the range of 3–10 nm depending upon the polymer composition and loading percentage. SANS and PALS reveal that nanopores (2–6 nm) are generated when the nanocomposites are heated to 500 °C. A transition from closed to interconnected pores is observed when the polymer loadings are increased. These porous materials exhibit high electrical breakdown field and good mechanical strength and are candidate materials for the next generation of ultralow- $k$  materials.

**Acknowledgment.** We would like to thank Robert Irwin for helping in the focus ion beam (FIB) and cross-sectional TEM studies. Andy Lovinger is acknowledged for the top-view TEM study. We are grateful to Pierre Wiltzius for the helpful discussion. We finally acknowledge the support of NIST, the U. S. Department of Commerce, and the National Science Foundation through Agreements DMR-9423101 and ECS-9732804, in providing neutron and positron research facilities, respectively, for this work.

CM010690L